Large Aperture, Holographically Corrected Membrane Telescope

(as appears in Optical Engineering, Vol. 41, No. 7, 1603-1607, July 2002)

Geoff P. Andersen (Member SPIE)
Randall J. Knize
USAF Academy
HQ USAFA/DFP, Suite 2A31
2354 Fairchild Dr.,
USAF Academy, CO 80840
Ph: 719-333-2829
Fax: 719-333-3182
Email: geoff.andersen@usafa.af.mil

Art Palisoc
Costas Cassapakis
L'Garde, Inc.
15181 Woodlawn Ave.,
Tustin, CA 92780-6487
Ph: 714-259-0771
Fax: 714-259-7822
Email: art_palisoc@lgarde.com

Abstract
We have constructed a 1m-diameter, holographically corrected membrane mirror telescope for optical imaging. Several thousand waves of surface error were removed using a corrective hologram, resulting in near diffraction-limited performance. A detailed discussion of the mirror, the corrective process and the performance of the final telescope are included.
Subject terms: Holography, lightweight telescopes, image correction, space optics

1. Introduction

The construction of large diameter (>10m), space-based optical systems will require new technologies in order to dramatically reduce construction and launch costs. With current lightweight composites, areal masses as small as ~5-10kg/m^2 are possible over smaller diameters[1-4]. However, the construction of a single, large primary for high-resolution imaging will require several smaller diameter mirror segments to be perfectly positioned and phased together in orbit. Our approach is to construct an ultra-lightweight membrane mirror that can be unfurled from a highly compact package to create a large monolithic primary. The distortions in the surface figure can then be removed using holographic correction techniques, to produce a diffraction-limited telescope operating over a narrow bandwidth. In this way, the areal density of the primary can be reduced by two to three orders of magnitude while also making it possible to construct mirrors up to 100m in diameter.

The basic holographic correction scheme[5-11], is shown in Fig. 1. A collimated source of laser light is incident on the membrane mirror (Fig. 1a). The reflected light comes to an aberrated focus before passing through a camera lens that produces a demagnified image of the primary onto the surface of the holographic medium. A hologram is recorded between this beam and a coherent, diffraction limited plane wave incident from an angle. On replay (Fig. 1b), light from a distant object is focused by the membrane mirror to reproduce the aberrated wave once more. At the hologram, this "object beam" will reconstruct an unaberrated plane wave that can be focused down to form a diffraction-limited image of the distant object. In this way we can use a small, inexpensive hologram to correct for distortions in a large aperture over a narrow bandwidth.

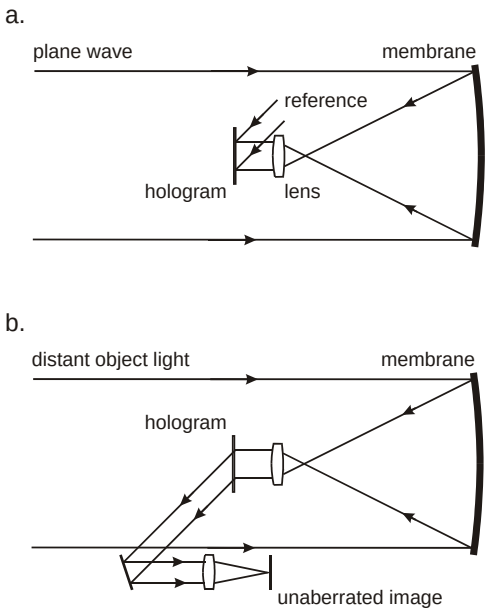

Fig. 1: The correction process. **a.** A hologram is recorded between an aberrated beam from the membrane mirror and a plane wave reference beam. **b.** Light from a distant object reconstructs an unaberrated beam.

The above scheme requires a diffraction-limited, plane wave with the same diameter as the membrane to be corrected. In our ground-based tests, this is achieved by using a high-quality collimating optic. In a space-based system, however, a distant point source of light will be used instead. The feasibility of such an approach has been discussed elsewhere[12]. A further consideration with this technique is that the hologram is a phase element, which applies a different absolute correction at different wavelengths. As such the diffraction-limited bandwidth depends on the magnitude of the initial aberrations and the desired final performance. The final wavefront aberration (ϕ_2) is related to the initial error (ϕ_1) and the recording and reconstruction wavelengths (λ_1 and λ_2 respectively) by:

$$\phi_2 = \frac{|\lambda_2 - \lambda_1|}{\lambda_2}\phi_1 \qquad (1)$$

2. Membrane mirror

A membrane mirror was constructed by L'Garde, Inc[13-16] from a sheet of 12.7μm thick Kapton-E (ρ_a = 17 g/m^2) with a 100nm vapor-deposited reflective aluminum layer (reflectivity ~90% @ 532nm). The membrane was cut into a 1.2m diameter circular disc that was then affixed to a 1.5x1.5m metal plate having a 1.1m diameter hole in the center. Bonded to the rear of the membrane were 166 tabs, 5mm in diameter, arranged in a hexagonal array. With the metal plate forming the front side of a box, Kevlar strings attached to the tabs could be pulled through to the back plate where they were fixed to a series of tension adjusters. By manipulating the tension in particular strings, the front surface could be made to deform into a concave surface with 166 dimples.

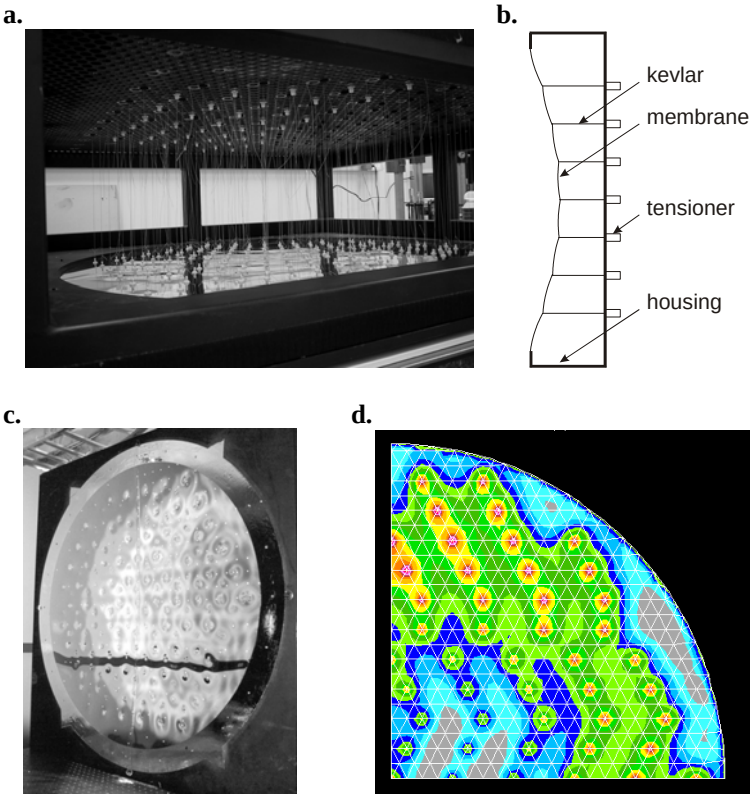

Fig. 2: The membrane mirror. **a.** The mirror is shown face-down with the strings attached to the back plate at the top of the image. **b.** A schematic of the mirror design. **c.** The mirror viewed from the side. **d.** A contour map of the expected mirror figure derived from finite element modeling, with each color representing 3.64μm increase in vertical displacement.

The initial surface figure was obtained by first placing a transparent membrane over the front of the reflective membrane with an airtight seal made on the surrounding metal plate. The space between the two membranes was pressurized until the reflective membrane had deformed to the desired radius of curvature. At this point the slack in Kevlar strings was taken up using the adjusters on the back plate. The air pressure was then released, and the transparent membrane removed. The figure of the reflective membrane was maintained by the tension in the strings. An image of the pulled-tabs

viewed between the two plates (with the mirror face-down) is shown in Fig. 2a, with a schematic of the mirror design in Fig. 2b.

We used the above technique to create a 1m-diameter mirror with a focal length of approximately 2.65m, as shown in Fig 2c. A finite element analysis (Fig. 2d) using in-house software[13] predicted that the surface error was 250μm rms (using 91 tabs) and 155μm rms (using 166 tabs). In an optical sense, however, the actual performance of this mirror will be worse than suggested by this number due to the extreme slopes of the mirror obtained close to the tab locations. When illuminated by a collimated beam, this mirror produces a focal "spot" over 100mm in diameter (Fig. 3a). This equates to a surface error of over 15,000 waves[17].

While the majority of our experiments were aimed at testing the possibility of correcting such a large, heavily aberrated membrane using holographic techniques, several factors in the mirror design are important. In order to record a hologram, the object cannot move by more than a fraction of the wavelength of light during exposure. For this reason, the membrane design required the heavy-duty metal housing to maintain a stable figure in the Earth environment. In practice, a space telescope based on this pulled-tab membrane design would be configured with a membrane backing panel and inflated, stiffened struts, making it orders of magnitude less massive. Furthermore, for perfect correction, the mirror must retain the same surface between recording and reconstruction, so no creep in the membrane material is permitted. We noticed no appreciable relaxation of the membrane surface over periods of days while the reconstruction was being analyzed, indicating a very stable figure.

3. Holographic correction

We used an experimental set-up similar to that shown in Fig. 1. Collimated light, produced with a parabolic mirror (D = 1m, f = 2.375m, 0.75λ rms), was directed onto the aberrated membrane primary. The focused light was captured by a camera lens (f = 85mm, F/1.2), which formed a 32mm-diameter image of the surface of the membrane mirror onto the holographic film. A hologram was recorded with a diffraction-limited, plane wave reference beam incident on the plate from an angle of approximately 48^{o} to the normal. The choice of this angle is not critical, but was the minimum angle for which the reference beam could clear the camera lens. Phase holograms were recorded using a continuous-wave, frequency-doubled Nd:YAG laser (λ = 532nm) on bleached Agfa 8E56 plate film. Typically phase holograms produced in such a medium can be expected to be 70-90% efficient[8-12], but due to the effect of low-frequency vibrations and air turbulence on the membrane, the actual efficiency was an order of magnitude lower than this.

After processing, the hologram was returned to the recording position for reconstruction. With the collimated light again reflected off the membrane mirror and through the secondary optics onto the hologram, the original reference beam was reconstructed. The fidelity of the reconstructed beam was then analyzed. Note that because the collimator is the illuminating source for recording and replay in an identical geometry, the 0.75 waves rms surface aberration will not be present on the corrected beam.

4. Results

The uncorrected focal spot is shown in Fig. 3a, contrast-enhanced in order to exaggerate the detail. Most of the intensity is contained within a 100mm diameter as shown, though some light is present at off-axis distances greater than 300mm due to the extreme mirror curvatures near the tab locations. Since the imaging lens was not large enough to capture all of the rays, portions of the mirror cannot be corrected. We estimate that the secondary gathers 20% of the light incident on the primary, which could be increased with an improved mirror figure. A copy of the hologram (Fig. 3b) indicates the areas of the mirror aperture that are imaged and corrected (in black). The fact that the aperture is not filled will lead to some degradation in the point spread function (PSF). From the image hologram we can model the expected PSF (Fig. 3c), which shows that although some contrast is lost, there will be little change in resolution compared to that of a filled aperture (Fig. 3d).

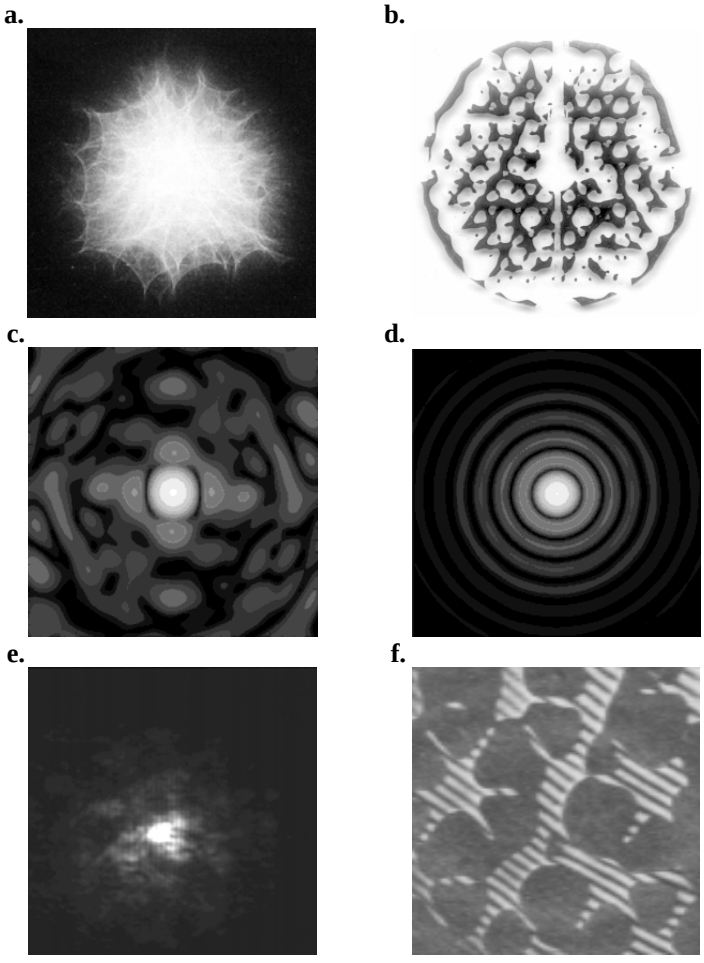

Fig. 3: a. A contrast-enhanced image of the focal spot from the uncorrected membrane mirror. **b.** A contact print of the image hologram. **c.** The point spread function (PSF) calculated from the image hologram (shown with logarithmic scaling). **d.** The PSF of a filled aperture with the same dimensions as the hologram (log scaling). **e.** The focal spot of the corrected beam. The box dimensions for images **a.** and **e.** are 140mm, 100μm respectively. **f.** A magnified portion of an interferogram after correction.

After correction, the reconstructed beam was focused by a 200mm achromat to produce the focus shown magnified in Fig. 3e, with a central maximum 7.5μm in diameter. The diffraction limited spot size for a filled aperture in this set-up would be 6.8μm. The fidelity of the reconstructed beam was further tested by forming an interference pattern with a plane wave, as shown in Fig. 3f. Straight fringes were achieved over the entire aperture indicating near diffraction-limited performance. For clarity, only a portion of the interferogram of the mirror aperture is shown.

To determine the imaging capability of the telescope, a 1951 USAF resolution test target was placed at the focus of the collimator, and illuminated with laser light passed through a moving diffuser. The reconstructed beam from the hologram was then focused to produce the image shown in Fig. 4a. Examination of the image shows that Group 6, Element 4 is resolved, indicating a telescope resolution of 90 line pairs per mm. The resolution limit for this configuration is Group 7, Element 2 (148 lppmm). In the case of both the interferogram and resolution test chart results, it was not possible to produce a "before" image due to the severity of the aberrations.

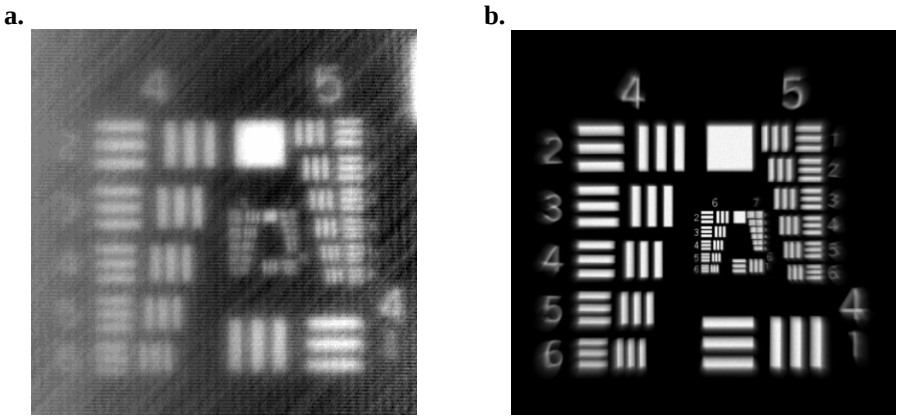

Fig. 4: Imaging. **a.** An image of a 1951 USAF resolution test target produced from the reconstructed beam. The image has been contrast enhanced for publication clarity. **b.** A simulation of the "best result".

Much of the residual blurring and loss of resolution in the imaging test was due to air turbulence and vibrational effects unrelated to the correction process, so the actual performance is expected to be better than measured. Furthermore, the limited field of view of the collimator results in the introduction of aberrations that degrades the quality of the image being projected onto the membrane mirror. The effect of these aberrations is shown in the computer-generated image, Fig. 4b. This can be thought of as the "best result" – and the image to which Fig. 4a should be compared. It is also important to note that the hologram is only correcting for a single point in the telescope field of view (the location of the initial laser point source). As such, the corrected primary will have very similar field of view characteristics to that of a perfect primary with the same dimensions[8].

A static hologram is used to apply a particular phase correction as originally recorded. If the mirror figure changes, there will be a residual aberration after correction, which is the

difference in the aberrations in the mirror. As a result, vibrations and turbulence in the lab limited the performance of our holographically corrected membrane telescope. A realtime correction system, incorporating either a dynamic holographic medium (such as photopolymers) or a post-hologram adaptive optics system, could be used to adjust for temporal changes[12]. We are currently conducting research into both techniques.

5. Conclusion

We have constructed a 1m-diameter membrane mirror, which was then holographically corrected. The primary has very low areal mass ($17g/m^2$) while being highly compactable and easily deployed in a space environment. While this mirror has over 10,000 waves surface error in the optical regime, it was still possible to achieve near diffraction-limited performance in a less than ideal, Earth environment. Future research is being conducted into improved mirror design and increased imaging performance.

Acknowledgements

We would like to acknowledge the Air Force Office of Scientific Research for their support of this research, as well as Mike DiVittorio at the US Naval Observatory.

References

1. P. C. Chen and R. C. Romeo, “Ultra lightweight precision optics technology,” Proc. SPIE 4003, 396-405 (2000).
2. P. C. Chen et al., “Advances in very lightweight composite mirror technology,” Opt. Eng. 39, 2320-2329 (2000).
3. B. Catanzaro et al., “UltraLITE glass/composite hybrid mirror,” Proc. SPIE 4013 663-671 (2000).
4. D. Baiocchi, J. H. Burge and B. Cuerden, “Demonstration of a 0.5-m ultralightweight mirror for use at geosynchronous orbit,” Proc. SPIE 4451 (2001).
5. Y. N. Denisyuk and S. I. Soskin, “Holographic correction of deformational aberrations of the main mirror of a telescope,” Opt. Spectrosc. 31, 535-538 (1971).
6. S. I. Soskin and Y. N. Denisyuk, “Holographic correction of optical-system aberrations caused by main-mirror deformation,” Opt. Spectrosc. 33, 544-545 (1972).
7. J. Munch, R. Wuerker and L. Heflinger, “Wideband holographic correction of an aberrated telescope objective,” Appl. Opt. 29, 2440-2445 (1990).
8. G. Andersen, Ph.D. Thesis, University of Adelaide, 1996.
9. G. Andersen, J. Munch and P. Veitch, “Compact, holographic correction of aberrated telescopes,” Appl. Opt. 36, 1427-1432 (1997).
10. R. B. Andreev *et al.* “Experimental realization of the laser telescope with the overall compensation for the distortions via phase conjugation,” Proc. SPIE 2478, 324-327 (1995).
11. G. Andersen and R. J. Knize, “Holographically corrected telescope for high bandwidth optical communications,” Appl. Opt. 38, 6833-6835 (1999).
12. G. Andersen and R. J. Knize, “Holographically corrected telescope with temporal update,” Proc. SPIE 4013, 587-594, (2000).

13. A. L. Palisoc and Y. Huang, “Design tool for inflatable space structures,” Am. Inst. Aero. Astro. 1378, 2922-2930 (1997).
14. C. G. Cassapakis, A. W. Love and A. L. Palisoc, “Inflatable space antennas – A brief overview,” Proc IEEE Aerospace Conference, (1998).
15. D. Lichodziejewski and C. Cassapakis, “Inflatable power antenna technology,” Am. Inst. Aero. Astro. 1074, 1-10 (1999).
16. A. B. Meinel and M. P. Meinel, “Inflatable membrane mirrors for optical passband imagery,” Opt. Eng. 39, 541-550 (2000).
17. J. L. Rayces, “Exact relation between wave aberration and ray aberration,” Opt. Acta 11, 85-88 (1965).